

1 **TLR9 mediated tumour-stroma interactions in human**
2 **papilloma virus (HPV)-positive head and neck squamous**
3 **cell carcinoma up-regulate PD-L1 and PD-L2**

4
5 **Paramita Baruah^{1,2*}, Jessica Bullenkamp², Philip O.G. Wilson³, Michael Lee¹,**
6 **Juan Carlos Kaski² and Ingrid E. Dumitriu^{2*}**

7
8 *Running title: TLR9 and PD-1/PD-L1/PD-L2 pathways in HNSCC*

9
10 ¹Department of ENT, St. George's Hospital NHS Trust London, UK, ²Molecular and
11 Clinical Sciences Research Institute, St. George's, University of London, London,
12 UK, ³Department of Pathology, St. George's Hospital NHS Trust London, UK

13
14
15 ***Correspondence:**

16 Corresponding authors: Paramita Baruah, paramita.baruah@nhs.net; and, Ingrid E.
17 Dumitriu, i.dumitriu@sgul.ac.uk; Molecular and Clinical Sciences Research Institute,
18 St. George's, University of London, Cranmer Terrace, SW17 0RE, London, UK;
19 phone +442087252808; fax +442087253328

20
21 **Keywords: fibroblasts, HNSCC, HPV, PD-1, PD-L1, PD-L2, TLR9**

22
23 **Word count: 8,209; 7 Figures; 1 Table**

24
25

26 **Abstract**

27 **Background:** The co-inhibitory receptor PD-1 is expressed in many tumours
28 including head and neck squamous cell carcinoma (HNSCC) and is an important
29 immunotherapy target. However, the role of PD-1 ligands, PD-L1 and particularly
30 PD-L2, in the tumour-stromal cell interactions that cause a tumour-permissive
31 environment in HNSCC is not completely understood and is the focus of our study.

32 **Methods:** Expression of PD-L1 and PD-L2 was analysed by immunohistochemistry
33 *in situ* in HNSCC tumour tissue. Co-cultures were established between stromal cells
34 (fibroblasts and macrophages) and human papilloma virus (HPV)-positive and HPV-
35 negative HNSCC cell lines (HNSCCs) and PD-1 ligands expression was analysed
36 using flow cytometry.

37 **Results:** PD-L1 and PD-L2 were expressed both in tumour cells and stroma in
38 HNSCC tissue *in situ*. *In vitro*, basal expression of PD-L1 and PD-L2 was low in
39 HNSCCs and high on fibroblasts and macrophages. Interestingly, HPV-positive but
40 not HPV-negative HNSCCs increased the expression of both PD-1 ligands on
41 fibroblasts upon co-culture. This effect was not observed with macrophages.
42 Conversely, both fibroblasts and macrophages increased PD-1 ligands on HPV-
43 positive HNSCCs, whilst this was not observed in HPV-negative HNSCCs. Crucially,
44 we demonstrate that up-regulation of PD-L1 and PD-L2 on fibroblasts by HPV-
45 positive HNSCCs is mediated via TLR9.

46 **Conclusions:** This work demonstrates in an *in vitro* model that HPV-positive
47 HNSCCs regulate PD-L1/2 expression on fibroblasts via TLR9. This may open novel
48 avenues to modulate immune checkpoint regulator PD-1 and its ligands by targeting
49 TLR9.

50

51 Introduction

52 Advanced stage head and neck squamous cell carcinoma (HNSCC) is treated with a
53 combination of surgery, radiotherapy and chemotherapy with considerable morbidity
54 and mortality. A significant advance in knowledge was the discovery that the
55 oncogenic human papilloma virus (HPV, subtypes 16 and 18) associates with 60-70%
56 of oro-pharyngeal cancer, a common HNSCC (Venuti *et al.*, 2004). Additionally, the
57 observation that HPV-positive HNSCC patients have a better prognosis than those
58 with HPV-negative HNSCC raises interesting questions about the immune response
59 to the HPV-antigen in HPV-positive HNSCC.

60 Circulating T cells specific for HPV with anti-tumour activity have been identified in
61 patients with HNSCC by us and others (Albers *et al.*, 2005; Baruah *et al.*, 2012),
62 indicating an immune response to HPV virus. However HNSCC develops and
63 progresses in spite of this because tumour antigen-specific T cells fail to eliminate the
64 tumour. We have previously shown that circulating HPV-antigen specific CD8⁺ T
65 cells in patients with p16-positive HNSCC express high levels of the co-inhibitory
66 receptor programmed cell death-1 (PD-1) (Baruah *et al.*, 2012), which may
67 compromise their cytotoxic function (Ahmadzadeh *et al.*, 2009). PD-1 is expressed by
68 activated T cells following antigen encounter and it limits the proliferation and
69 cytokine production of effector T cells (Okazaki *et al.*, 2013; Nishimura *et al.*, 1999).
70 The inhibitory actions of PD-1 are triggered by interaction with its ligands, PD-1
71 ligand 1 (PD-L1, B7-H1 or CD274) and PD-L2 (B7-DC or CD273). These ligands
72 compete for binding to PD-1 and their expression pattern is complex. PD-L1 is
73 constitutively expressed by immune cells (T cells, B cells, dendritic cells,
74 macrophages) and also by non-haematopoietic parenchymal cells in many tissues
75 (Nguyen and Ohashi, 2015). In contrast, PD-L2 expression is reportedly restricted to
76 antigen presenting cells (dendritic cells, macrophages and B cells) (Nguyen and
77 Ohashi, 2015).

78 PD-L1 is also expressed in many tumours (Strome *et al.*, 2003; Wintterle *et al.*, 2003;
79 Zou and Chen, 2008; Dong *et al.*, 2002; Konishi *et al.*, 2004), and more recently
80 tumour PD-L2 expression has been described (Yearley *et al.*, 2017). Some of the
81 mechanisms proposed to drive expression of PD-L1 in tumours include interferon- γ
82 (IFN- γ) produced by tumour infiltrating lymphocytes, genomic alterations, and
83 activation of oncogenic signaling pathways (George *et al.*, 2017; Howitt *et al.*, 2016;
84 Kataoka *et al.*, 2016; Lastwika *et al.*, 2016; Loi *et al.*, 2016; Topalian *et al.*, 2012; Wilke
85 *et al.*, 2011). However, additional mechanisms are likely to exist. PD-1/PD-L1 axis is
86 a major immune checkpoint important in the prognosis of several solid tumours
87 (melanoma, hepatocellular carcinoma and more recently HNSCC) (Gao *et al.*, 2009;
88 Hino *et al.*, 2010; Lyford-Pike *et al.*, 2013; Velcheti *et al.*, 2014) and is being clinically
89 targeted for immunotherapy (Ansell *et al.*, 2015; Brahmer *et al.*, 2012; Hamid *et al.*,
90 2013; Topalian *et al.*, 2014; Wolchok *et al.*, 2013). Recent work on antibodies
91 targeting PD-1 in advanced melanoma has yielded encouraging improvement in
92 survival (Topalian *et al.*, 2014) and clinical trials are currently investigating the
93 efficacy of anti-PD-1 and anti-PD-L1 monoclonal antibodies in recurrent and/or
94 metastatic HNSCC (Forster and Devlin, 2018; Pai *et al.*, 2016; Saada-Bouzid *et al.*,
95 2019).

96 Stromal cells such as tumour-associated macrophages and fibroblasts have important
97 roles in generating an immunosuppressive tumour milieu (Junttila and de Sauvage,
98 2013). The role of PD-L1 and in particular PD-L2 in the tumour-permissive function

99 of stromal cells in HPV-positive and HPV-negative HNSCC is yet to be completely
100 understood. In this study we investigate whether interactions between tumour and
101 stromal cells influence the expression of PD-1 ligands in HNSCC. We demonstrate
102 that PD-L1 and PD-L2 are expressed in both tumour and stromal cells in HNSCC
103 tissue from treatment-naïve patients. We present novel data that HPV-positive but not
104 HPV-negative HNSCC cell lines (HNSCCs) increase PD-L1 and PD-L2 expression
105 on fibroblasts. Of note, we demonstrate that the up-regulation of PD-L1 and PD-L2
106 on fibroblasts driven by HPV-positive HNSCCs is mediated via TLR9 as it was
107 abrogated by the TLR9-specific antagonist ODN TTAGGG. Interestingly,
108 chloroquine - an endosomal TLR inhibitor - selectively abrogated PD-L2 up-
109 regulation. This is the first report demonstrating TLR9 involvement in regulation of
110 PD-L1 and PD-L2 expression in the interaction between HPV-positive HNSCCs and
111 stromal cells. Our findings have potential implications for PD-1/PD-L1/PD-L2
112 immune checkpoint modulation in HPV-positive HNSCC by unveiling TLR9 as an
113 alternative target.
114

115 **Materials and methods**

116 **HNSCC tissue samples**

117 Immunohistochemistry was performed on tumour biopsies from nine treatment-naive
118 HNSCC patients with newly diagnosed cancers. Patients' characteristics are
119 summarized in **Table 1**. To reduce the impact of inflammatory comorbidities on the
120 expression of PD-1 and its ligands, strict exclusion criteria were applied and patients
121 with co-existing inflammatory disorders such as autoimmune diseases, diabetes, renal
122 failure and cardiac disease were excluded from the study. The study was carried out in
123 accordance with the recommendations of the Research Ethics Committee London-
124 Chelsea who approved the study; all study subjects gave written informed consent in
125 accordance with the Declaration of Helsinki.

126 **Cell lines**

127 The human head and neck squamous cell carcinoma lines (HNSCCs) UPCI-SCC-099
128 (SCC099) and UPCI-SCC-154 (SCC154) were purchased from DSMZ
129 (Braunschweig, Germany). The SCC099 line was HPV-negative while the SCC154
130 line was HPV-positive. HNSCCs were maintained in Dulbecco's modified Eagle
131 medium (DMEM, Sigma, #D6546) supplemented with 100 U/ml penicillin, 100
132 µg/ml streptomycin, 15 mM L-glutamine, 1 x non-essential amino acids and 10%
133 heat-inactivated fetal calf serum (FCS, Corning) (culture medium). Primary human BJ
134 fibroblasts (ATCC CRL-2522) were cultured in culture medium without non-essential
135 amino acids.

136 **Primary human monocyte-derived macrophage differentiation**

137 Peripheral blood mononuclear cells (PBMCs) were isolated from healthy blood
138 donors by density gradient centrifugation using Histopaque (Sigma-Aldrich; #10771).
139 Monocytes were isolated by adherence to tissue culture-treated 12-well plates by
140 plating $3-5 \times 10^6$ PBMCs per well in Iscove's modified Dulbecco's medium (IMDM,
141 Sigma-Aldrich; #I3390) supplemented with 100 U/ml penicillin, 100 µg/ml
142 streptomycin, 15 mM L-glutamine and 5% heat-inactivated pooled human serum
143 (Lonza; #14-490E). Following incubation for 1 hour at 37°C non-adhering cells were
144 removed and culture medium was replaced. The culture medium was exchanged after
145 3-4 days and monocytes were differentiated into macrophages by 6-7 days culture at
146 37°C. Macrophage differentiation was routinely verified by staining with monoclonal
147 antibodies against CD14 (APC; BD Biosciences; #555399) and CD68 (FITC;
148 #562117; BD Biosciences).

149 **Co-cultures**

150 1×10^5 BJ fibroblasts were co-cultured with SCC099 or SCC154 cell lines (HNSCCs)
151 at 1:1 ratio in culture medium. Fibroblasts or HNSCCs cultured alone were used as
152 controls. Similar co-cultures were set up between primary human macrophages and
153 HNSCCs. Briefly, the culture medium was removed from differentiated macrophages
154 and 1.5×10^5 SCC099 or SCC154 cells were added in culture medium. Macrophages
155 or HNSCCs cultured alone were used as controls. Co-cultures were incubated for 48
156 hours prior to analysis of PD-1 ligand expression by flow cytometry. In addition to
157 direct co-cultures, cells (HNSCC, fibroblasts, or macrophages) were treated with
158 conditioned media and PD-L1/PD-L2 expression was assessed after 48 hours by flow
159 cytometry. Conditioned media were prepared from supernatants of confluent cultures
160 of HNSCCs, fibroblasts and macrophages filtered through 0.2 µm pore membranes to
161 remove viable and apoptotic cells. Where indicated, cells were cultured in the
162 presence of ODN TTAGGG (3.9 µM, InvivoGen; #tlrl-ttag151), chloroquine (10 µM,

163 InvivoGen; #tlrl-chq) or neutralizing antibodies against interferon- γ (IFN- γ , 5 ug/ml,
 164 R&D Systems; MAB285), tumour necrosis factor- α (TNF- α , 5 ug/ml, R&D Systems;
 165 #MAB610) and CD81/TAPA-1 (5 ug/ml, Abcam; #ab35026).

166 **Cell line authentication**

167 UPCI-SCC-099 (SCC099) and UPCI-SCC-154 (SCC154) HNSCC cell lines were
 168 received directly from DSMZ (Braunschweig, Germany), which used short tandem
 169 repeat (STR) DNA profiling for their authentication. Primary BJ human fibroblasts
 170 were obtained from ATCC, which used STR profiling for their characterisation. SCCs
 171 and fibroblasts were passaged for less than 3 months and therefore re-authentication
 172 was not required.

173 **Immunohistochemistry**

174 The following primary antibodies were used: mouse monoclonal CD4 (#NCL-L-CD4-
 175 368); mouse monoclonal CD8 (#NCL-L-CD8-4B11); mouse monoclonal CD68
 176 (#NCL-L-CD68) and mouse monoclonal CD163 (#NCL-L-CD163) (all from
 177 Novocastra, Leica Biosystems); rabbit polyclonal anti-inducible nitric oxide synthase
 178 (iNOS, Abcam; #ab3523); goat polyclonal PD-1 (#AF1086) and goat polyclonal PD-
 179 L2 (#AF1224) (both R&D Systems) and mouse monoclonal CD274 (PD-L1)
 180 (Biolegend; #329702). Paraffin sections of tumour tissue were cut at 4 μ m and heated
 181 for 45 minutes at 60°C prior to staining. Heat antigen retrieval was carried out using
 182 Epitope Retrieval Solution 1 (for all antibodies except CD68), pH 6 or Epitope
 183 Retrieval Solution 2 (CD68), pH 9 at 100°C for 20 or 30mins, according to the
 184 antibody. Antibodies were diluted 1:50 (CD8, PD-1, PD-L1) or 1:100 for the
 185 remaining antibodies, and incubated for 15 minutes. Negative controls used antibody
 186 diluent in place of primary antibody. Visualisation for mouse monoclonal antibodies
 187 was carried out using the Bond Polymer Refine Detection kit, an HRP-conjugated
 188 3,3'-diaminobenzidine (DAB) detection system (Leica Biosystems; #DS9800).
 189 Visualisation for goat polyclonal antibodies was by Bond Intense R kit, a
 190 Biotin/streptavidin HRP-conjugated DAB detection system, supplied by Leica
 191 Microsystems and secondary antibody biotinylated rabbit anti-goat (Dako; #E0466).
 192 All immunohistochemistry staining was carried out using Bond III Fully automated
 193 staining system and associated reagents, supplied by Leica Microsystems. Images
 194 were captured with a Hamamatsu Nanozoomer RS2.0 slide scanner, equipped with an
 195 Olympus objective (20x and 40x magnification) using the NDP.scan software. Images
 196 were generated using the NDP.view 2 software.

197 **Flow cytometry analysis**

198 For detection of PD-L1 and PD-L2, fibroblasts and HNSCC cell lines (HNSCCs)
 199 cultured alone or in co-culture were detached by incubation with Trypsin/EDTA
 200 (Sigma-Aldrich) at 37°C, followed by washes in culture medium. Macrophages and
 201 HNSCCs cultured alone or in co-culture were collected by incubation in PBS
 202 containing 5 mM EDTA and 0.2% w/v bovine serum albumin for 15 minutes on ice
 203 and gentle scraping. Cells were washed several times in PBS with 2% FCS and
 204 stained for surface expression of epithelial cell adhesion molecule (EpCAM) (APC;
 205 R&D Systems; #FAB9601A) to distinguish HNSCCs from fibroblasts and
 206 macrophages. Additionally, cells were stained with PE-conjugated monoclonal
 207 antibodies against PD-L1 (#12-5983-42) and PD-L2 (#12-5888-42) (both
 208 eBioscience) or PE-conjugated isotype control antibodies (BD Biosciences; #555749).
 209 Initial experiments for detection of PD-L1 expression used a mouse anti-human-PD-
 210 L1 antibody (Biolegend; #329702) followed by staining with PE-conjugated goat
 211 anti-mouse antibody (Sigma-Aldrich; P9287). For macrophage-HNSCCs co-cultures,

212 7-AAD (BD Biosciences; #559925) was used to exclude dead cells from the analysis.
213 Samples were acquired on a FACSCalibur (BD Biosciences) flow cytometer and data
214 analysis was performed using FlowJo software version 7. Mean fluorescence intensity
215 (MFI) was calculated by subtracting the MFI of samples stained with PE-conjugated
216 isotype control from the MFI of samples stained with PD-L1 and PD-L2, respectively.
217 MFI for samples indirectly stained with PD-L1/GAM-PE was adjusted to match MFI
218 of samples stained with PE-conjugated PD-L1.

219 **Quantification of cytokines in culture supernatants**

220 Supernatants from co-cultures of fibroblasts and HPV-positive HNSCCs were stored
221 frozen until quantification of IFN- γ and TNF- α by DuoSet ELISA (R&D Systems;
222 #DY285, IFN- γ ; #DY210, TNF- α).

223 **Statistical analysis**

224 One-way ANOVA with Bonferroni post-test for multiple comparisons and unpaired
225 two-tailed Student's *t*-test were performed using GraphPad Prism assuming
226 independent samples and normal distribution (as indicated in the Figure legends).
227 Probability (p) values of < 0.05 were considered statistically significant.
228

229 Results

230 PD-L1 and PD-L2 are expressed both in tumour cells and stroma in HNSCC 231 tissue

232 We examined expression of PD-L1 and PD-L2 in nine treatment-naïve HNSCC
233 tumour tissue samples using immunohistochemistry (clinical details in **Table 1**). PD-
234 L1 was expressed in all tissue samples and was present both in tumour cells and
235 stromal tissue (**Figure 1**). Similarly, PD-L2 was also present in all tissue samples
236 examined and both tumour cells and stroma expressed PD-L2 *in situ* (**Figure 1**).
237 Semi-quantitative analysis did not reveal differences in the expression of PD-1
238 ligands in p16-positive and p16-negative HNSCC tissue (**Figure 1**). We next
239 examined PD-1 expression in the HNSCC tissue. An infiltrate of PD-1⁺ cells was
240 noted in all HNSCC samples (**Figure 1**). Moreover, all HNSCC samples also
241 exhibited CD8⁺ cell infiltration (**Figure 1**). Fewer PD-1⁺ and CD8⁺ cells were present
242 in p16-negative samples (**Figure 1**). Compared to CD8 expression, relatively lower
243 numbers of CD4⁺ cells were found in HNSCC tumour tissue (**Figure 1**). We also
244 examined macrophage presence in HNSCC tumour tissue using CD68 (pan-
245 macrophage marker), iNOS (M1 marker) and CD163 (M2 marker). CD68⁺ and
246 CD163⁺ macrophages were noted in all HNSCC, while iNOS-positive macrophages
247 were not identified (**Figure 2**).

248 HPV-positive HNSCCs up-regulate PD-L1 and PD-L2 expression on fibroblasts

249 As we found that PD-1 ligands were expressed in both tumour and stroma of HNSCC
250 tissues, we examined if interaction between HNSCC tumour cells and fibroblasts
251 could influence expression of PD-1 ligands. We therefore tested the effect of HPV-
252 positive (SCC154) and HPV-negative (SCC099) HNSCC cell lines (HNSCCs) on
253 PD-1 ligand expression on BJ fibroblasts in an *in vitro* co-culture system. Fibroblasts
254 expressed high baseline levels of PD-L1 and PD-L2, whilst HPV-positive and HPV-
255 negative HNSCCs expressed low levels (**Figure 3A and B**). Interestingly, expression
256 of PD-L1 on fibroblasts increased significantly upon co-culture with HPV-positive
257 HNSCCs (**Figure 3C and E**, $p < 0.0001$). In contrast, HPV-negative HNSCCs
258 decreased PD-L1 on fibroblasts (**Figure 3D and E**). The same pattern was noted for
259 PD-L2 expression on fibroblasts: HPV-positive HNSCCs significantly increased PD-
260 L2 levels (**Figure 3C and E**, $p < 0.0001$), whilst HPV-negative HNSCCs decreased
261 PD-L2 (**Figure 3D and E**).

262 Fibroblasts up-regulate PD-L1 and PD-L2 expression in HPV-positive HNSCCs

263 As HPV-positive HNSCCs up-regulated PD-1 ligands on BJ fibroblasts, we also
264 examined whether fibroblasts had a reciprocal effect on PD-1 ligands expression on
265 HNSCCs. Interaction with fibroblasts in co-culture significantly increased PD-L1 and
266 PD-L2 expression on HPV-positive HNSCCs (**Figure 3F and G**, $p < 0.0001$). In
267 contrast, PD-L1 and PD-L2 expression on HPV-negative HNSCCs did not change
268 following co-culture with fibroblasts (**Figure 3H and I**).

269 Macrophages up-regulate PD-L1 and PD-L2 on HPV-positive HNSCCs

270 Macrophages are another important constituent of tumour stroma and therefore we
271 tested the effect of HNSCCs on PD-1 ligand expression by macrophages. Primary
272 peripheral blood monocyte-derived human macrophages expressed both PD-L1 and
273 PD-L2 (**Figure 4A**). In contrast to our findings on fibroblasts, co-culture with HPV-
274 positive HNSCCs did not increase PD-L1 and PD-L2 expression on macrophages
275 (**Figure 4B and D**). Similarly, HPV-negative HNSCCs did not affect PD-1 ligands

276 expression on macrophages (**Figure 4C and D**). We also examined the effect of
277 macrophages on PD-1 ligand expression by HNSCCs. PD-L1 and PD-L2 expression
278 on HPV-positive HNSCCs increased significantly following direct co-culture with
279 macrophages (**Figure 4E and F**), although the effect was more marked for PD-L1
280 than for PD-L2. In contrast, macrophages did not alter PD-1 ligands expression on
281 HPV-negative HNSCCs (**Figure 4G and H**).

282 **Conditioned medium from HPV-positive HNSCCs up-regulates PD-L1 and PD-** 283 **L2 on fibroblasts**

284 We next analysed the mechanisms underlying the up-regulation of PD-1 ligands on
285 fibroblasts upon co-culture with HPV-positive HNSCCs. To determine whether this
286 was contact dependent or mediated via soluble factors, fibroblasts were cultured
287 either with HPV-positive HNSCCs or with conditioned medium (supernatant) from
288 these cells (details in Methods). Treatment with conditioned medium induced
289 significant PD-L1 up-regulation on fibroblasts (**Figure 5A and B**). However, the
290 effect of conditioned medium was smaller than that observed with direct co-culture:
291 whilst direct co-culture with HPV-positive HNSCCs resulted in four-fold up-
292 regulation of PD-L1, conditioned medium induced a 1.6 fold increase (**Figure 5A**
293 **and B**). Next we analysed the effect of conditioned medium on PD-L2 expression.
294 Significant up-regulation of PD-L2 was observed on fibroblasts cultured with
295 conditioned medium from HPV-positive HNSCCs (**Figure 5A and B**). Of note, the
296 effect of conditioned medium on PD-L2 expression on fibroblasts was similar to that
297 induced by direct co-culture with HPV-positive HNSCCs. As fibroblasts increased
298 PD-1 ligand expression on HPV-positive HNSCCs in co-culture (**Figure 3F and G**),
299 we tested whether this was also the case with conditioned medium from fibroblasts.
300 Conditioned medium from cultures of fibroblasts did not alter PD-L1 and PD-L2
301 ligand expression on HPV-positive HNSCCs (**Figure 5C-D**). We also assessed the
302 effect of HPV-positive HNSCCs conditioned medium on macrophages and found no
303 change on PD-L1 and PD-L2 expression (**Figure 5E**). Similarly, conditioned medium
304 from macrophages had no effect on PD-L1 and PD-L2 expression on HPV-positive
305 HNSCCs (**Figure 5F**).

306 **The up-regulation of PD-1 ligands on fibroblasts induced by HPV-positive** 307 **HNSCCs is not mediated by interferon- γ (IFN- γ), tumour necrosis factor- α** 308 **(TNF- α) or tetraspanin CD81**

309 Inflammatory cytokines such as IFN- γ have been proposed to mediate PD-L1 up-
310 regulation on several cell types (Topalian *et al.*, 2012; Wilke *et al.*, 2011). Moreover,
311 tumour-infiltrating lymphocytes were proposed to induce PD-L1 expression in
312 HNSCC via IFN- γ (Lyford-Pike *et al.*, 2013). We therefore tested supernatants from
313 fibroblasts co-cultured with HPV-positive HNSCCs or with conditioned medium from
314 these cells for inflammatory cytokines. No IFN- γ or TNF- α was present in
315 supernatants from fibroblasts cultured alone or in the presence of HPV-positive
316 HNSCCs or conditioned medium from these cells (**Figure 6A**). In addition, blocking
317 IFN- γ or TNF- α with neutralizing antibodies did not have any impact on PD-L1 and
318 PD-L2 up-regulation on fibroblasts cultured with HPV-positive HNSCCs or
319 conditioned medium (**Figure 6B-E**). We also investigated whether transfer of PD-1
320 ligands via microvesicles derived from HPV-positive HNSCCs could account for PD-
321 L1 and PD-L2 increase on fibroblasts. We therefore targeted tetraspanin CD81
322 (TAPA-1), which is a common component of tetraspanin-enriched microdomains in
323 the membrane of microvesicles and has been implicated in the entry of viruses like

324 HPV and hepatitis C virus in epithelial cells (Raposo and Stoorvogel, 2013). Blocking
325 antibodies against tetraspanin CD81 did not inhibit PD-L1 and PD-L2 up-regulation
326 by fibroblasts co-cultured with HPV-positive HNSCCs or conditioned medium from
327 these cells (**Figure 6F-G**).

328 **The up-regulation of PD-L1 and PD-L2 on fibroblasts by HPV-positive HNSCCs**
329 **is mediated via Toll-like receptor-9 (TLR9)**

330 Toll-like receptors (TLR) have been implicated in up-regulation of PD-L1 in antigen
331 presenting cells (Wolfe *et al.*, 2011). Endosomal TLR9 is a primary sensor for
332 bacterial and viral DNA (Kawai and Akira, 2010). As HPV is a double stranded DNA
333 virus we next investigated whether TLR9 was involved in PD-L1 and PD-L2
334 expression by fibroblasts co-cultured with HPV-positive HNSCCs. For this purpose
335 we used the oligonucleotide ODN TTAGGG (A151), which is a specific antagonist of
336 human TLR9 (Kaminski *et al.*, 2013; Krieg *et al.*, 1998). Notably, ODN TTAGGG
337 abrogated the up-regulation of both PD-L1 and PD-L2 in fibroblasts co-cultured with
338 HPV-positive HNSCCs (**Figure 7A and C**), whilst it had no effect on the baseline
339 expression of PD-1 ligands on fibroblasts (**Figure 7D and E**). Furthermore, ODN
340 TTAGGG significantly inhibited the up-regulation of PD-L1 and PD-L2 in fibroblasts
341 cultured with conditioned medium from HPV-positive HNSCCs (**Figure 7B and C**).
342 As fibroblasts increased the expression of PD-1 ligands on HPV-positive HNSCCs
343 (**Figure 3F and G**), we tested whether this effect was also mediated by TLR9.
344 Indeed, ODN TTAGGG hindered the up-regulation of PD-L1 and PD-L2 on HPV-
345 positive HNSCCs cultured with fibroblasts (**Figure 7F and G**). In addition to ODN
346 TTAGGG, we tested another TLR9 inhibitor, chloroquine, which works by blocking
347 endosomal acidification that is required for optimal TLR9 activation, and by
348 inhibiting the binding of DNA to TLR9 (Kuznik *et al.*, 2011; Rutz *et al.*, 2004). As
349 observed with ODN TTAGGG, chloroquine inhibited the up-regulation of PD-L2 by
350 fibroblasts cultured either directly with HPV-positive HNSCCs or with conditioned
351 medium from these cells (**Figure 7H-J**). In contrast to ODN TTAGGG, chloroquine
352 did not affect PD-L1 expression on fibroblasts in these experiments (**Figure 7H-J**).
353 Moreover, chloroquine had no effect on the baseline expression of PD-L1 and PD-L2
354 by fibroblasts (**Figure 7K and L**). In contrast to ODN TTAGGG, chloroquine also
355 did not affect the fibroblast-induced up-regulation of PD-L1 and PD-L2 on HPV-
356 positive HNSCCs (**Figure 7M and N**).

357

358 **Discussion**

359 This work investigated the role of the inhibitory PD-1 pathway with focus on PD-L1
 360 and PD-L2 in the stromal microenvironment in HNSCC. Here we show that PD-L1
 361 and PD-L2 are expressed in both tumour cells and stroma *in situ* in treatment-naïve
 362 primary HSNCC. Of note, we demonstrate that HPV-positive HNSCC cell lines
 363 (HNSCCs) up-regulate both PD-L1 and PD-L2 expression on fibroblasts *in vitro* via a
 364 TLR9-dependent mechanism. To the best of our knowledge this is the first report
 365 identifying TLR9 as a new regulator of PD-1 ligand expression in fibroblasts in the
 366 context of tumour-stroma interaction. Our novel results suggest that HPV-positive
 367 HNSCC enlist fibroblasts and generate a tumour-permissive microenvironment via
 368 TLR9-mediated engagement of PD-1/PD-L1/PD-L2 pathways.

369 PD-L1 and PD-L2 are members of the B7 superfamily of co-stimulatory/co-inhibitory
 370 molecules (Ceeraz *et al.*, 2013) and bind to PD-1 expressed on T cells. In immune
 371 responses to tumours, PD-1 engagement on T cells is responsible for switching T
 372 lymphocytes off and preventing robust anti-tumour activity (Ahmadzadeh *et al.*,
 373 2009). Thereby PD-1 ligands have pivotal roles in maintaining an immunosuppressive
 374 microenvironment in tumours. In comparison to PD-L1, little information is available
 375 on PD-L2 expression in HNSCC. We show that both PD-1 ligands (PD-L1 and PD-
 376 L2) are expressed in HNSCC tissue *in situ* and are present in both tumour and stromal
 377 cells. Our findings on PD-L2 expression are in agreement with a recent study on
 378 tissue expression of PD-L2 from 40 HNSCC patients (Yearley *et al.*, 2017). This study
 379 also suggested that PD-L2 expression is a significant predictor of clinical response to
 380 pembrolizumab (an anti-PD-1 checkpoint inhibitor) and progression-free survival,
 381 independent of PD-L1 status in HNSCC (Yearley *et al.*, 2017). These data highlight a
 382 role for PD-L2 in HNSCC and suggest that PD-L2, in addition to PD-L1, has a role in
 383 tumour-stroma interactions in HNSCC *in vivo*. However, very little is known about
 384 the mechanisms regulating PD-L1 and in particular PD-L2 expression in HNSCC
 385 tumour and stroma.

386 We found constitutive expression of PD-L1 and PD-L2 in human primary BJ
 387 fibroblasts. Expression of PD-L2 has been previously described in fibroblasts from
 388 human intestinal mucosa (Pinchuk *et al.*, 2008) and from human lung cancers
 389 (Nazareth *et al.*, 2007), although its role on fibroblasts is not completely understood.
 390 Notably, we found that co-culture with the HPV-positive HNSCC cell line (HNSCCs)
 391 significantly increased the expression of PD-L1 and PD-L2 on fibroblasts. This effect
 392 of HPV-positive HNSCCs was restricted to fibroblasts as it was not observed on
 393 primary human macrophages. Of note, fibroblasts and macrophages also increased the
 394 expression of PD-L1 and PD-L2 on HPV-positive HNSCCs. These results suggest a
 395 bi-directional interaction between HPV-positive tumour cells and stromal cells,
 396 resulting in an overall up-regulation of both PD-L1 and PD-L2.

397 A novel facet of our work unveils TLR9 as a receptor mediating the up-regulation of
 398 PD-L1 and PD-L2 on fibroblasts following interaction with HPV-positive HNSCCs.
 399 We found that ODN TTAGGG, a specific antagonist of TLR9, abrogated the up-
 400 regulation of both PD-L1 and PD-L2. Interestingly, chloroquine, another TLR9
 401 inhibitor blocked PD-L2 up-regulation but had no effect on PD-L1. These findings
 402 may be explained by different mechanisms employed by ODN TTAGGG and
 403 chloroquine in TLR9 inhibition. TLR9 is an endosomal pattern recognition receptor
 404 for unmethylated 2'-deoxyribo(cytidine-phosphate-guanosine) (CpG) oligonucleotide

405 (ODN) DNA motifs preferentially found in bacterial and viral DNA and rare in
406 mammalian cells (Kawai and Akira, 2010). ODN TTAGGG is believed to interfere
407 with CpG ODN colocalisation with TLR9 in endosomes (Gursel *et al.*, 2003), whilst
408 chloroquine hinders TLR9 activation by inhibiting endosomal acidification and
409 blocking nucleic acid binding to TLR9 (Kuznik *et al.*, 2011; Rutz *et al.*, 2004). The
410 different effects of ODN TTAGGG and chloroquine on PD-L1 and PD-L2 suggest
411 further complexities in TLR9 regulation of PD-1 ligand expression that warrant
412 investigation. In contrast to the effect on fibroblasts, HPV-positive HNSCCs did not
413 up-regulate PD-L1 or PD-L2 on monocyte-derived macrophages. This may be due to
414 low TLR9 expression in human monocyte-derived macrophages (Kierner *et al.*, 2009;
415 O'Mahony *et al.*, 2008).

416 Our *in vitro* results show a clear influence of HPV status on the expression of PD-L1
417 and PD-L2 by fibroblasts coming into contact with HNSCC cell lines. This is in
418 keeping with *in situ* findings by Lyford-Pike *et al.* that PD-L1 expression was more
419 common in HPV-positive HNSCC tissue (70%, n=14/20 of their cohort) compared to
420 HPV-negative samples (29%, n=2/10) (Lyford-Pike *et al.*, 2013). In our study,
421 immunohistochemistry staining did not reveal differences in PD-L1 and PD-L2
422 expression in treatment-naïve p16-positive compared to p16-negative HNSCC tissue
423 samples (**Figure 1**), which may be due to the smaller sample size. Of note, a recent
424 RNASeq gene expression profiling in more than 500 treatment-naïve HNSCC tissue
425 samples did not identify differences in PD-L1 expression in HPV-positive and HPV-
426 negative HNSCC, even though IFN- γ (an inducer of PD-L1) was significantly higher
427 in the HPV-positive group (Gameiro *et al.*, 2018). It is possible that in the tumour
428 microenvironment, up-regulation of PD-1 ligands is influenced by multiple factors in
429 addition to HPV. Quantification of PD-1 ligands solely in fibroblasts in tumour tissue
430 *in situ* presents major challenges as no specific markers are available that can reliably
431 identify fibroblasts *in situ*.

432 A limitation of our study is the use of an *in vitro* co-culture system to dissect the
433 effect of the interactions between HNSCC cell lines and stromal cells on the
434 expression of PD-1 ligands. For ethical and feasibility reasons, the fibroblasts used in
435 this study were primary established cell lines and macrophages were generated from
436 peripheral blood monocytes of normal donors. To investigate fibroblasts and
437 macrophages directly isolated from HNSCC tumour tissue is challenging because of
438 limited amounts of fresh tumour tissue available for research. Moreover, methods
439 used to isolate macrophages and fibroblasts from tumour tissue and propagate these
440 cells *in vitro* alter the phenotype and function of these cells.

441 Our results show that PD-1/PD-L1 and PD-1/PD-L2 pathways are important in the
442 bidirectional interaction between tumour cells and stromal cells in HNSCC and could
443 shape the anti-tumour immune response. We propose TLR9 as a new regulator of the
444 interaction between HPV-positive HNSCCs and stromal cells, specifically fibroblasts,
445 which controls PD-L1 and PD-L2 expression. Further dissection of TLR9's role in
446 modulation of PD-1 ligands could reveal novel strategies to target PD-1 pathways and
447 improve clinical outcomes in HPV-positive HNSCC.
448

449 **Acknowledgements**

450 We are grateful to Professor Christopher Gregory for the human macrophages
451 differentiation protocol. We are very grateful to all the patients for their participation
452 in the study. Immunohistochemistry images were captured in the Image Resource
453 Facility (IRF), St. George's University of London. We are grateful to IRF staff for
454 advice on using the Hamamatsu slide scanner and image generation.

455 **Author contributions statement**

456 PB designed and directed the study, recruited the patients, collected clinical data,
457 designed experiments, analysed data and wrote the manuscript. ID designed and
458 supervised the study, designed and performed experiments, analysed data and wrote
459 the manuscript. JB designed and performed *in vitro* experiments, analysed data and
460 edited the manuscript. PW analysed data and provided critical discussion. ML
461 provided access to patients and critical discussion. JK provided access to vital
462 resources.

463 **Conflict of interest statement**

464 The authors declare no potential conflicts of interest.

465 **Funding disclosure**

466 This work was funded by the Royal College of Surgeons of Edinburgh (grant no.
467 SRG/10/033 and SRG/12/059 to PB) and the St George's Hospital Charity (to PB and
468 IED). Work in IED's laboratory is funded by the British Heart Foundation (grant no.
469 PG/10/50/28434, PG/13/24/30115, PG/14/18/30724, PG/17/15/32845 to IED).

470 **Materials and data policies**

471 The generated datasets have been included in the manuscript and the supplementary
472 material. The raw data supporting the conclusions of this manuscript will be made
473 available by the authors, without undue reservation, to any qualified researcher.

474

475 **References**

476

477 Ahmadzadeh, M., Johnson, L.A., Heemskerk, B., Wunderlich, J.R., Dudley, M.E.,
 478 White, D.E., and Rosenberg, S.A. (2009). Tumor antigen-specific CD8 T cells
 479 infiltrating the tumor express high levels of PD-1 and are functionally impaired.
 480 *Blood* 114, 1537-1544.

481 Albers, A., Abe, K., Hunt, J., Wang, J., Lopez-Albaitero, A., Schaefer, C., Gooding,
 482 W., Whiteside, T.L., Ferrone, S., Deleo, A., and Ferris, R.L. (2005). Antitumor
 483 activity of human papillomavirus type 16 E7-specific T cells against virally
 484 infected squamous cell carcinoma of the head and neck. *Cancer Res* 65, 11146-
 485 11155.

486 Ansell, S.M., Lesokhin, A.M., Borrello, I., Halwani, A., Scott, E.C., Gutierrez, M.,
 487 Schuster, S.J., Millenson, M.M., Cattry, D., Freeman, G.J., Rodig, S.J., Chapuy,
 488 B., Ligon, A.H., Zhu, L., Grosso, J.F., Kim, S.Y., Timmerman, J.M., Shipp,
 489 M.A., and Armand, P. (2015). PD-1 blockade with nivolumab in relapsed or
 490 refractory Hodgkin's lymphoma. *N Engl J Med* 372, 311-319.

491 Baruah, P., Lee, M., Odutoye, T., Williamson, P., Hyde, N., Kaski, J.C., and
 492 Dumitriu, I.E. (2012). Decreased levels of alternative co-stimulatory receptors
 493 OX40 and 4-1BB characterise T cells from head and neck cancer patients.
 494 *Immunobiology* 217, 669-675.

495 Brahmer, J.R., Tykodi, S.S., Chow, L.Q., Hwu, W.J., Topalian, S.L., Hwu, P., Drake,
 496 C.G., Camacho, L.H., Kauh, J., Odunsi, K., Pitot, H.C., Hamid, O., Bhatia, S.,
 497 Martins, R., Eaton, K., Chen, S., Salay, T.M., Alaparthi, S., Grosso, J.F.,
 498 Korman, A.J., Parker, S.M., Agrawal, S., Goldberg, S.M., Pardoll, D.M., Gupta,
 499 A., and Wigginton, J.M. (2012). Safety and activity of anti-PD-L1 antibody in
 500 patients with advanced cancer. *N Engl J Med* 366, 2455-2465.

501 Ceeraz, S., Nowak, E.C., and Noelle, R.J. (2013). B7 family checkpoint regulators in
 502 immune regulation and disease. *Trends Immunol* 34, 556-563.

503 Dong, H., Strome, S.E., Salomao, D.R., Tamura, H., Hirano, F., Flies, D.B., Roche,
 504 P.C., Lu, J., Zhu, G., Tamada, K., Lennon, V.A., Celis, E., and Chen, L. (2002).
 505 Tumor-associated B7-H1 promotes T-cell apoptosis: a potential mechanism of
 506 immune evasion. *Nat Med* 8, 793-800.

507 Forster, M.D., and Devlin, M.J. (2018). Immune Checkpoint Inhibition in Head and
 508 Neck Cancer. *Front Oncol* 8, 310.

509 Gameiro, S.F., Ghasemi, F., Barrett, J.W., Koropatnick, J., Nichols, A.C., Mymryk,
 510 J.S., and Maleki Vareki, S. (2018). Treatment-naive HPV+ head and neck cancers
 511 display a T-cell-inflamed phenotype distinct from their HPV- counterparts that
 512 has implications for immunotherapy. *Oncoimmunology* 7, e1498439.

513 Gao, Q., Wang, X.Y., Qiu, S.J., Yamato, I., Sho, M., Nakajima, Y., Zhou, J., Li, B.Z.,
 514 Shi, Y.H., Xiao, Y.S., Xu, Y., and Fan, J. (2009). Overexpression of PD-L1
 515 significantly associates with tumor aggressiveness and postoperative recurrence
 516 in human hepatocellular carcinoma. *Clin Cancer Res* 15, 971-979.

517 George, J., Saito, M., Tsuta, K., Iwakawa, R., Shiraishi, K., Scheel, A.H., Uchida, S.,
 518 Watanabe, S.I., Nishikawa, R., Noguchi, M., Peifer, M., Jang, S.J., Petersen, I.,
 519 Buttner, R., Harris, C.C., Yokota, J., Thomas, R.K., and Kohno, T. (2017).
 520 Genomic Amplification of CD274 (PD-L1) in Small-Cell Lung Cancer. *Clin*
 521 *Cancer Res* 23, 1220-1226.

522 Gursel, I., Gursel, M., Yamada, H., Ishii, K.J., Takeshita, F., and Klinman, D.M.
 523 (2003). Repetitive elements in mammalian telomeres suppress bacterial DNA-
 524 induced immune activation. *J Immunol* 171, 1393-1400.

- 525 Hamid, O., Robert, C., Daud, A., Hodi, F.S., Hwu, W.J., Kefford, R., Wolchok, J.D.,
526 Hersey, P., Joseph, R.W., Weber, J.S., Dronca, R., Gangadhar, T.C., Patnaik, A.,
527 Zarour, H., Joshua, A.M., Gergich, K., Ellassaiss-Schaap, J., Algazi, A., Mateus,
528 C., Boasberg, P., Tumeh, P.C., Chmielowski, B., Ebbinghaus, S.W., Li, X.N.,
529 Kang, S.P., and Ribas, A. (2013). Safety and tumor responses with
530 lambrolizumab (anti-PD-1) in melanoma. *N Engl J Med* 369, 134-144.
- 531 Hino, R., Kabashima, K., Kato, Y., Yagi, H., Nakamura, M., Honjo, T., Okazaki, T.,
532 and Tokura, Y. (2010). Tumor cell expression of programmed cell death-1 ligand
533 1 is a prognostic factor for malignant melanoma. *Cancer* 116, 1757-1766.
- 534 Howitt, B.E., Sun, H.H., Roemer, M.G., Kelley, A., Chapuy, B., Aviki, E., Pak, C.,
535 Connelly, C., Gjini, E., Shi, Y., Lee, L., Viswanathan, A., Horowitz, N., Neuberg,
536 D., Crum, C.P., Lindeman, N.L., Kuo, F., Ligon, A.H., Freeman, G.J., Hodi, F.S.,
537 Shipp, M.A., and Rodig, S.J. (2016). Genetic Basis for PD-L1 Expression in
538 Squamous Cell Carcinomas of the Cervix and Vulva. *JAMA Oncol* 2, 518-522.
- 539 Junttila, M.R., and De Sauvage, F.J. (2013). Influence of tumour micro-environment
540 heterogeneity on therapeutic response. *Nature* 501, 346-354.
- 541 Kaminski, J.J., Schattgen, S.A., Tzeng, T.C., Bode, C., Klinman, D.M., and
542 Fitzgerald, K.A. (2013). Synthetic oligodeoxynucleotides containing suppressive
543 TTAGGG motifs inhibit AIM2 inflammasome activation. *J Immunol* 191, 3876-
544 3883.
- 545 Kataoka, K., Shiraishi, Y., Takeda, Y., Sakata, S., Matsumoto, M., Nagano, S.,
546 Maeda, T., Nagata, Y., Kitanaka, A., Mizuno, S., Tanaka, H., Chiba, K., Ito, S.,
547 Watatani, Y., Kakiuchi, N., Suzuki, H., Yoshizato, T., Yoshida, K., Sanada, M.,
548 Itonaga, H., Imaizumi, Y., Totoki, Y., Munakata, W., Nakamura, H., Hama, N.,
549 Shide, K., Kubuki, Y., Hidaka, T., Kameda, T., Masuda, K., Minato, N.,
550 Kashiwase, K., Izutsu, K., Takaori-Kondo, A., Miyazaki, Y., Takahashi, S.,
551 Shibata, T., Kawamoto, H., Akatsuka, Y., Shimoda, K., Takeuchi, K., Seya, T.,
552 Miyano, S., and Ogawa, S. (2016). Aberrant PD-L1 expression through 3'-UTR
553 disruption in multiple cancers. *Nature* 534, 402-406.
- 554 Kawai, T., and Akira, S. (2010). The role of pattern-recognition receptors in innate
555 immunity: update on Toll-like receptors. *Nat Immunol* 11, 373-384.
- 556 Kiemer, A.K., Senaratne, R.H., Hoppstadter, J., Diesel, B., Riley, L.W., Tabeta, K.,
557 Bauer, S., Beutler, B., and Zuraw, B.L. (2009). Attenuated activation of
558 macrophage TLR9 by DNA from virulent mycobacteria. *J Innate Immun* 1, 29-
559 45.
- 560 Konishi, J., Yamazaki, K., Azuma, M., Kinoshita, I., Dosaka-Akita, H., and
561 Nishimura, M. (2004). B7-H1 expression on non-small cell lung cancer cells and
562 its relationship with tumor-infiltrating lymphocytes and their PD-1 expression.
563 *Clin Cancer Res* 10, 5094-5100.
- 564 Krieg, A.M., Wu, T., Weeratna, R., Efler, S.M., Love-Homan, L., Yang, L., Yi, A.K.,
565 Short, D., and Davis, H.L. (1998). Sequence motifs in adenoviral DNA block
566 immune activation by stimulatory CpG motifs. *Proc Natl Acad Sci U S A* 95,
567 12631-12636.
- 568 Kuznik, A., Bencina, M., Svajger, U., Jeras, M., Rozman, B., and Jerala, R. (2011).
569 Mechanism of endosomal TLR inhibition by antimalarial drugs and
570 imidazoquinolines. *J Immunol* 186, 4794-4804.
- 571 Lastwika, K.J., Wilson, W., 3rd, Li, Q.K., Norris, J., Xu, H., Ghazarian, S.R.,
572 Kitagawa, H., Kawabata, S., Taube, J.M., Yao, S., Liu, L.N., Gills, J.J., and
573 Dennis, P.A. (2016). Control of PD-L1 Expression by Oncogenic Activation of

- 574 the AKT-mTOR Pathway in Non-Small Cell Lung Cancer. *Cancer Res* 76, 227-
575 238.
- 576 Loi, S., Dushyanthen, S., Beavis, P.A., Salgado, R., Denkert, C., Savas, P., Combs,
577 S., Rimm, D.L., Giltnane, J.M., Estrada, M.V., Sanchez, V., Sanders, M.E.,
578 Cook, R.S., Pilkinton, M.A., Mallal, S.A., Wang, K., Miller, V.A., Stephens, P.J.,
579 Yelensky, R., Doimi, F.D., Gomez, H., Ryzhov, S.V., Darcy, P.K., Arteaga, C.L.,
580 and Balko, J.M. (2016). RAS/MAPK Activation Is Associated with Reduced
581 Tumor-Infiltrating Lymphocytes in Triple-Negative Breast Cancer: Therapeutic
582 Cooperation Between MEK and PD-1/PD-L1 Immune Checkpoint Inhibitors.
583 *Clin Cancer Res* 22, 1499-1509.
- 584 Lyford-Pike, S., Peng, S., Young, G.D., Taube, J.M., Westra, W.H., Akpeng, B.,
585 Bruno, T.C., Richmon, J.D., Wang, H., Bishop, J.A., Chen, L., Drake, C.G.,
586 Topalian, S.L., Pardoll, D.M., and Pai, S.I. (2013). Evidence for a role of the PD-
587 1:PD-L1 pathway in immune resistance of HPV-associated head and neck
588 squamous cell carcinoma. *Cancer Res* 73, 1733-1741.
- 589 Nazareth, M.R., Broderick, L., Simpson-Abelson, M.R., Kelleher, R.J., Jr., Yokota,
590 S.J., and Bankert, R.B. (2007). Characterization of human lung tumor-associated
591 fibroblasts and their ability to modulate the activation of tumor-associated T
592 cells. *J Immunol* 178, 5552-5562.
- 593 Nguyen, L.T., and Ohashi, P.S. (2015). Clinical blockade of PD1 and LAG3--
594 potential mechanisms of action. *Nat Rev Immunol* 15, 45-56.
- 595 Nishimura, H., Nose, M., Hiai, H., Minato, N., and Honjo, T. (1999). Development of
596 lupus-like autoimmune diseases by disruption of the PD-1 gene encoding an
597 ITIM motif-carrying immunoreceptor. *Immunity* 11, 141-151.
- 598 O'mahony, D.S., Pham, U., Iyer, R., Hawn, T.R., and Liles, W.C. (2008). Differential
599 constitutive and cytokine-modulated expression of human Toll-like receptors in
600 primary neutrophils, monocytes, and macrophages. *Int J Med Sci* 5, 1-8.
- 601 Okazaki, T., Chikuma, S., Iwai, Y., Fagarasan, S., and Honjo, T. (2013). A rheostat
602 for immune responses: the unique properties of PD-1 and their advantages for
603 clinical application. *Nat Immunol* 14, 1212-1218.
- 604 Pai, S.I., Zandberg, D.P., and Strome, S.E. (2016). The role of antagonists of the PD-
605 1:PD-L1/PD-L2 axis in head and neck cancer treatment. *Oral Oncol* 61, 152-158.
- 606 Pinchuk, I.V., Saada, J.I., Beswick, E.J., Boya, G., Qiu, S.M., Mifflin, R.C., Raju,
607 G.S., Reyes, V.E., and Powell, D.W. (2008). PD-1 ligand expression by human
608 colonic myofibroblasts/fibroblasts regulates CD4+ T-cell activity.
609 *Gastroenterology* 135, 1228-1237, 1237 e1221-1222.
- 610 Raposo, G., and Stoorvogel, W. (2013). Extracellular vesicles: exosomes,
611 microvesicles, and friends. *J Cell Biol* 200, 373-383.
- 612 Rutz, M., Metzger, J., Gellert, T., Luppa, P., Lipford, G.B., Wagner, H., and Bauer, S.
613 (2004). Toll-like receptor 9 binds single-stranded CpG-DNA in a sequence- and
614 pH-dependent manner. *Eur J Immunol* 34, 2541-2550.
- 615 Saada-Bouزيد, E., Peyrade, F., and Guigay, J. (2019). Immunotherapy in recurrent
616 and or metastatic squamous cell carcinoma of the head and neck. *Curr Opin*
617 *Oncol* 31, 146-151.
- 618 Strome, S.E., Dong, H., Tamura, H., Voss, S.G., Flies, D.B., Tamada, K., Salomao,
619 D., Chevillat, J., Hirano, F., Lin, W., Kasperbauer, J.L., Ballman, K.V., and Chen,
620 L. (2003). B7-H1 blockade augments adoptive T-cell immunotherapy for
621 squamous cell carcinoma. *Cancer Res* 63, 6501-6505.

- 622 Topalian, S.L., Drake, C.G., and Pardoll, D.M. (2012). Targeting the PD-1/B7-
623 H1(PD-L1) pathway to activate anti-tumor immunity. *Curr Opin Immunol* 24,
624 207-212.
- 625 Topalian, S.L., Sznol, M., McDermott, D.F., Kluger, H.M., Carvajal, R.D., Sharfman,
626 W.H., Brahmer, J.R., Lawrence, D.P., Atkins, M.B., Powderly, J.D., Leming,
627 P.D., Lipson, E.J., Puzanov, I., Smith, D.C., Taube, J.M., Wigginton, J.M.,
628 Kollia, G.D., Gupta, A., Pardoll, D.M., Sosman, J.A., and Hodi, F.S. (2014).
629 Survival, durable tumor remission, and long-term safety in patients with
630 advanced melanoma receiving nivolumab. *J Clin Oncol* 32, 1020-1030.
- 631 Velcheti, V., Schalper, K.A., Carvajal, D.E., Anagnostou, V.K., Syrigos, K.N., Sznol,
632 M., Herbst, R.S., Gettinger, S.N., Chen, L., and Rimm, D.L. (2014). Programmed
633 death ligand-1 expression in non-small cell lung cancer. *Lab Invest* 94, 107-116.
- 634 Venuti, A., Badaracco, G., Rizzo, C., Mafera, B., Rahimi, S., and Vigili, M. (2004).
635 Presence of HPV in head and neck tumours: high prevalence in tonsillar
636 localization. *J Exp Clin Cancer Res* 23, 561-566.
- 637 Wilke, C.M., Wei, S., Wang, L., Kryczek, I., Kao, J., and Zou, W. (2011). Dual
638 biological effects of the cytokines interleukin-10 and interferon-gamma. *Cancer*
639 *Immunol Immunother* 60, 1529-1541.
- 640 Wintterle, S., Schreiner, B., Mitsdoerffer, M., Schneider, D., Chen, L., Meyermann,
641 R., Weller, M., and Wiendl, H. (2003). Expression of the B7-related molecule
642 B7-H1 by glioma cells: a potential mechanism of immune paralysis. *Cancer Res*
643 63, 7462-7467.
- 644 Wolchok, J.D., Kluger, H., Callahan, M.K., Postow, M.A., Rizvi, N.A., Lesokhin,
645 A.M., Segal, N.H., Ariyan, C.E., Gordon, R.A., Reed, K., Burke, M.M.,
646 Caldwell, A., Kronenberg, S.A., Agunwamba, B.U., Zhang, X., Lowy, I.,
647 Inzunza, H.D., Feely, W., Horak, C.E., Hong, Q., Korman, A.J., Wigginton, J.M.,
648 Gupta, A., and Sznol, M. (2013). Nivolumab plus ipilimumab in advanced
649 melanoma. *N Engl J Med* 369, 122-133.
- 650 Wolfle, S.J., Strebosky, J., Bartz, H., Sahr, A., Arnold, C., Kaiser, C., Dalpke, A.H.,
651 and Heeg, K. (2011). PD-L1 expression on tolerogenic APCs is controlled by
652 STAT-3. *Eur J Immunol* 41, 413-424.
- 653 Yearley, J.H., Gibson, C., Yu, N., Moon, C., Murphy, E., Juco, J., Lunceford, J.,
654 Cheng, J., Chow, L.Q.M., Seiwert, T.Y., Handa, M., Tomassini, J.E., and
655 Mcclanahan, T. (2017). PD-L2 Expression in Human Tumors: Relevance to Anti-
656 PD-1 Therapy in Cancer. *Clin Cancer Res* 23, 3158-3167.
- 657 Zou, W., and Chen, L. (2008). Inhibitory B7-family molecules in the tumour
658 microenvironment. *Nat Rev Immunol* 8, 467-477.
659

660 **Figure legends**

661 **Figure 1. PD-L1, PD-L2, PD-1, CD8 and CD4 expression in p16-positive and**
 662 **p16-negative HNSCC.** PD-L1, PD-L2, PD-1, CD8 and CD4 expression was assessed
 663 in tumour biopsy tissue from five p16-positive and four p16-negative HNSCC
 664 patients using immuno-histochemistry (details in Methods). Representative staining
 665 (scale bars, 100 μ m) and cumulative data of marker expression (grading scale PD-
 666 L1/PD-L2: 1, low; 2, moderate; 3 high expression; grading scale PD-1, CD8, CD4: 1,
 667 <50 cells/field; 2, 50-150 cells/field; 3, >150 cells/field)

668 **Figure 2. CD68, CD163 and iNOS expression in p16-positive and p16-negative**
 669 **HNSCC.** Macrophage marker expression was assessed in tumour biopsy tissue from
 670 five p16-positive and four p16-negative HNSCC patients using immuno-
 671 histochemistry. Representative staining (scale bars, 100 μ m) and cumulative data of
 672 marker expression (grading scale: 1, <50 cells/field; 2, 50-100 cells/field; 3, >100
 673 cells/field)

674 **Figure 3. HPV-positive HNSCCs increase PD-L1 and PD-L2 on fibroblasts.** PD-
 675 L1 and PD-L2 expression on primary BJ human fibroblasts, HPV-positive (SCC154)
 676 and HPV-negative (SCC099) HNSCC cell lines (HNSCCs) was detected by flow
 677 cytometry. Illustrative histograms (A) show PD-L1 and PD-L2 expression on
 678 fibroblasts (black histograms), HPV-positive (red histograms) or HPV-negative (blue
 679 histograms) HNSCCs. Graphs show PD-L1 and PD-L2 expression (mean \pm SEM; n=5)
 680 in fibroblasts, HPV-positive and HPV-negative HNSCCs (B). Fibroblasts were
 681 cultured alone or co-cultured in direct contact (direct) with HPV-positive (SCC154)
 682 or HPV-negative (SCC099) HNSCCs. Fibroblasts were identified in co-cultures by
 683 lack of EpCAM expression. Illustrative histograms show PD-L1 and PD-L2
 684 expression on fibroblasts cultured alone (black histograms) or co-cultured directly
 685 with HPV-positive SCC154 (C; red histograms) or HPV-negative SCC099 (D; blue
 686 histograms). Graphs show PD-L1 and PD-L2 expression (mean \pm SEM; n=5) on
 687 fibroblasts cultured alone (w/o) or co-cultured directly with HNSCC cells (E). HPV-
 688 positive (SCC154) or HPV-negative (SCC099) HNSCCs were cultured alone or co-
 689 cultured in direct contact (direct) with fibroblasts. HNSCCs were identified in co-
 690 cultures by EpCAM expression. Illustrative histograms show PD-L1 and PD-L2
 691 expression on HPV-positive SCC154 cultured alone (black histograms) or co-cultured
 692 directly with fibroblasts (F; red histograms). Graphs show PD-L1 and PD-L2
 693 expression (mean \pm SEM; n=4) on HPV-positive SCC154 cultured alone or co-cultured
 694 directly with fibroblasts (G). Illustrative histograms show PD-L1 and PD-L2
 695 expression on HPV-negative SCC099 cultured alone (black histograms) or co-
 696 cultured directly with fibroblasts (H; blue histograms). Graphs show PD-L1 and PD-
 697 L2 expression (mean \pm SEM; n=4) on HPV-negative SCC099 cultured alone or co-
 698 cultured directly with fibroblasts (I). * p<0.05; ** p<0.01; **** p<0.0001; ns, not
 699 significant (one-way ANOVA with Bonferroni correction for multiple comparisons)
 700 Numbers adjacent to plots represent MFI values; dashed histograms show control
 701 staining with isotype-matched antibodies. MFI=mean fluorescence intensity

702 **Figure 4. PD-L1 and PD-L2 expression in co-cultures of macrophages and HPV-**
 703 **positive or HPV-negative HNSCCs.** Macrophages were cultured alone (w/o) or co-
 704 cultured in direct contact (direct) with HPV-positive (SCC154) or HPV-negative
 705 (SCC099) HNSCC cell lines (HNSCCs). Illustrative histograms show PD-L1 and PD-
 706 L2 expression on macrophages cultured alone (A; black histograms). Macrophages
 707 were identified in co-cultures by lack of EpCAM expression. Illustrative histograms

708 show PD-L1 and PD-L2 expression on macrophages cultured alone (black
 709 histograms) or co-cultured directly with HPV-positive SCC154 (**B**; red histograms) or
 710 HPV-negative SCC099 (**C**; blue histograms). Graphs show PD-L1 and PD-L2
 711 expression (mean±SEM; n=4) on macrophages cultured alone (w/o) or co-cultured
 712 directly with HNSCCs (**D**). HPV-positive (SCC154) or HPV-negative (SCC099)
 713 HNSCCs were cultured alone or co-cultured in direct contact (direct) with
 714 macrophages. HNSCCs were identified in co-cultures by EpCAM expression.
 715 Illustrative histograms show PD-L1 and PD-L2 expression on HPV-positive SCC154
 716 cultured alone (black histograms) or co-cultured directly with macrophages (**E**; red
 717 histograms). Graphs show PD-L1 and PD-L2 expression (mean±SEM; n=3) on HPV-
 718 positive SCC154 cultured alone or co-cultured directly with macrophages (**F**).
 719 Illustrative histograms show PD-L1 and PD-L2 expression on HPV-negative SCC099
 720 cultured alone (black histograms) or co-cultured directly with macrophages (**G**; blue
 721 histograms). Graphs show PD-L1 and PD-L2 expression (mean±SEM; n=3) on HPV-
 722 negative SCC099 cultured alone or co-cultured directly with macrophages (**H**). *
 723 p<0.05; ** p<0.01; ns, not significant (**D**: one-way ANOVA with Bonferroni
 724 correction for multiple comparisons; **F**, **H**: unpaired two-tailed Student's t test)
 725 Numbers adjacent to plots represent MFI values; dashed histograms show control
 726 staining with isotype-matched antibodies. MFI=mean fluorescence intensity

727 **Figure 5. Conditioned medium from HPV-positive HNSCCs up-regulates PD-L1**
 728 **and PD-L2 on fibroblasts.** Fibroblasts were cultured alone or co-cultured in direct
 729 contact with HPV-positive SCC154 (direct) or with conditioned medium from HPV-
 730 positive SCC154 (CM). Illustrative histograms show PD-L1 and PD-L2 expression on
 731 fibroblasts cultured alone (black histograms) or co-cultured with conditioned medium
 732 from HPV-positive SCC154 (**A**; red histograms). Graphs show PD-L1 and PD-L2
 733 expression (mean±SEM; n=13) on fibroblasts cultured alone (w/o), co-cultured
 734 directly with HPV-positive SCC154 (direct) or with conditioned medium from HPV-
 735 positive SCC154 (CM) (**B**). HPV-positive (SCC154) HNSCCs were cultured alone or
 736 co-cultured in direct contact with fibroblasts (Fibro direct) or with conditioned
 737 medium from fibroblasts (Fibro CM). Illustrative histograms show PD-L1 and PD-L2
 738 expression on HPV-positive SCC154 cultured alone (black histograms) or co-cultured
 739 with conditioned medium from fibroblasts (**C**; red histograms). Graphs show PD-L1
 740 and PD-L2 expression (mean±SEM; n=4) on HPV-positive SCC154 cultured alone
 741 (w/o), co-cultured directly with fibroblasts (Fibro direct) or with conditioned medium
 742 from fibroblasts (Fibro CM) (**D**). Macrophages were cultured alone (w/o) or co-
 743 cultured in direct contact with HPV-positive SCC154 (direct) or with conditioned
 744 medium from HPV-positive SCC154 (CM). Graphs show PD-L1 and PD-L2
 745 expression (mean±SEM; n=3) on macrophages for the indicated conditions (**E**). HPV-
 746 positive SCC154 HNSCCs were cultured alone (w/o) or co-cultured in direct contact
 747 with macrophages (MFs direct) or with conditioned medium from macrophages (MFs
 748 CM). Graphs show PD-L1 and PD-L2 expression (mean±SEM; n=2) on HPV-positive
 749 SCC154 HNSCCs for the indicated conditions (**F**).** p<0.01; **** p<0.0001; ns, not
 750 significant (one-way ANOVA with Bonferroni correction for multiple comparisons)
 751 Numbers adjacent to plots represent MFI values; dashed histograms show control
 752 staining with isotype-matched antibodies. MFI=mean fluorescence intensity

753 **Figure 6. Blockade of IFN- γ , TNF- α or CD81 does not affect PD-L1 and PD-L2**
 754 **up-regulation by HPV-positive HNSCCs.** Fibroblasts were cultured alone (w/o) or
 755 co-cultured in direct contact with HPV-positive SCC154 (SCC154 direct) or with
 756 conditioned medium from HPV-positive SCC154 (SCC154 CM) as indicated. Graphs

757 (A) show IFN- γ and TNF- α levels in culture supernatants (mean \pm SEM; n=4). The
 758 dashed red line indicates the lowest value (15.6 pg/ml) of the dynamic range for the
 759 ELISA assays used. Neutralising antibodies anti-IFN- γ (B, C), anti-TNF- α (D, E) or
 760 anti-CD81 (F, G) were added to the cultures as indicated. Illustrative histograms
 761 show PD-L1 and PD-L2 expression on fibroblasts cultured alone (black histograms),
 762 co-cultured directly with HPV-positive SCC154 or with conditioned medium from
 763 HPV-positive SCC154 alone (red histograms) or in the presence of blocking
 764 antibodies (green histograms). Graphs show PD-L1 and PD-L2 expression
 765 (mean \pm SEM; n=3) on fibroblasts for the indicated treatments. ns, not significant (one-
 766 way ANOVA with Bonferroni correction for multiple comparisons) Numbers
 767 adjacent to plots represent MFI values; dashed histograms show control staining with
 768 isotype-matched antibodies. MFI=mean fluorescence intensity

769 **Figure 7. The TLR9 antagonists ODN TTAGGG and chloroquine inhibit PD-1**
 770 **ligands up-regulation on fibroblasts co-cultured with HPV-positive HNSCCs.**
 771 Fibroblasts were cultured alone (w/o) or co-cultured in direct contact with HPV-
 772 positive SCC154 (SCC154 direct) or with conditioned medium from HPV-positive
 773 SCC154 (SCC154 CM) in the presence or absence of the TLR9 antagonists ODN
 774 TTAGGG (ODN) or chloroquine (CHQ). Illustrative histograms show PD-L1 and
 775 PD-L2 expression on fibroblasts cultured alone (black histograms), co-cultured
 776 directly with HPV-positive SCC154 (red histograms) or co-cultured directly with
 777 HPV-positive SCC154 in the presence of ODN (A) or CHQ (H) (green histograms).
 778 Illustrative histograms show PD-L1 and PD-L2 expression on fibroblasts cultured
 779 alone (black histograms), cultured with conditioned medium from HPV-positive
 780 SCC154 (red histograms) or with conditioned medium from HPV-positive SCC154 in
 781 the presence of ODN (B) or CHQ (I) (green histograms). Graphs show PD-L1 and
 782 PD-L2 expression (mean \pm SEM; n=6) on fibroblasts for the indicated treatments (C
 783 and J). Illustrative histograms show PD-L1 and PD-L2 expression on fibroblasts
 784 cultured alone (black histograms) or in the presence of ODN (D) or CHQ (K) (green
 785 histograms). Graphs show PD-L1 and PD-L2 expression (mean \pm SEM; n=4) on
 786 fibroblasts for the indicated treatments (E and L). HPV-positive SCC154 were
 787 cultured alone or co-cultured in direct contact (direct) with fibroblasts in the presence
 788 or absence of TLR9 inhibitor ODN TTAGGG (ODN) or chloroquine (CHQ).
 789 Illustrative histograms show PD-L1 and PD-L2 expression on HPV-positive SCC154
 790 cultured alone (black histograms), co-cultured directly with fibroblasts alone (red
 791 histograms), or co-cultured directly with fibroblasts in the presence of ODN (F) or
 792 CHQ (M) (green histograms). Graphs show PD-L1 and PD-L2 expression
 793 (mean \pm SEM; n=6) on HPV-positive SCC154 cultured alone or for the indicated co-
 794 culture conditions (G and N). * p<0.05; ** p<0.01; **** p<0.0001; ns, not
 795 significant (one-way ANOVA with Bonferroni correction for multiple comparisons)
 796 Numbers adjacent to plots represent MFI values; dashed histograms show control
 797 staining with isotype-matched antibodies. MFI=mean fluorescence intensity
 798

Table 1. Demographic characteristics of head and neck cancer patients

Patient	Age	Gender	Tumour site	TNM	p16
P1	61	F	Tonsil	T1N2bM0	Positive
P2	72	M	Tonsil/BOT	T4N2bM0	Positive
P3	62	M	Tonsil	T1N2aM0	Positive
P4	60	M	Tonsil	T3N0M0	Positive
P5	50	M	PFS/PCA	T4N0M0	Positive
P6	49	F	Uvula	T1N0M0	Negative
P7	83	M	PFS/PCA	T4N0M0	Negative
P8	50	F	BOT	T4N2cM0	Negative
P9	60	M	Tonsil/BOT	T4N2bM0	Negative

Abbreviations: BOT=base of tongue; PCA=postcricoid area; PFS=pyriform sinus

799

Figure 1

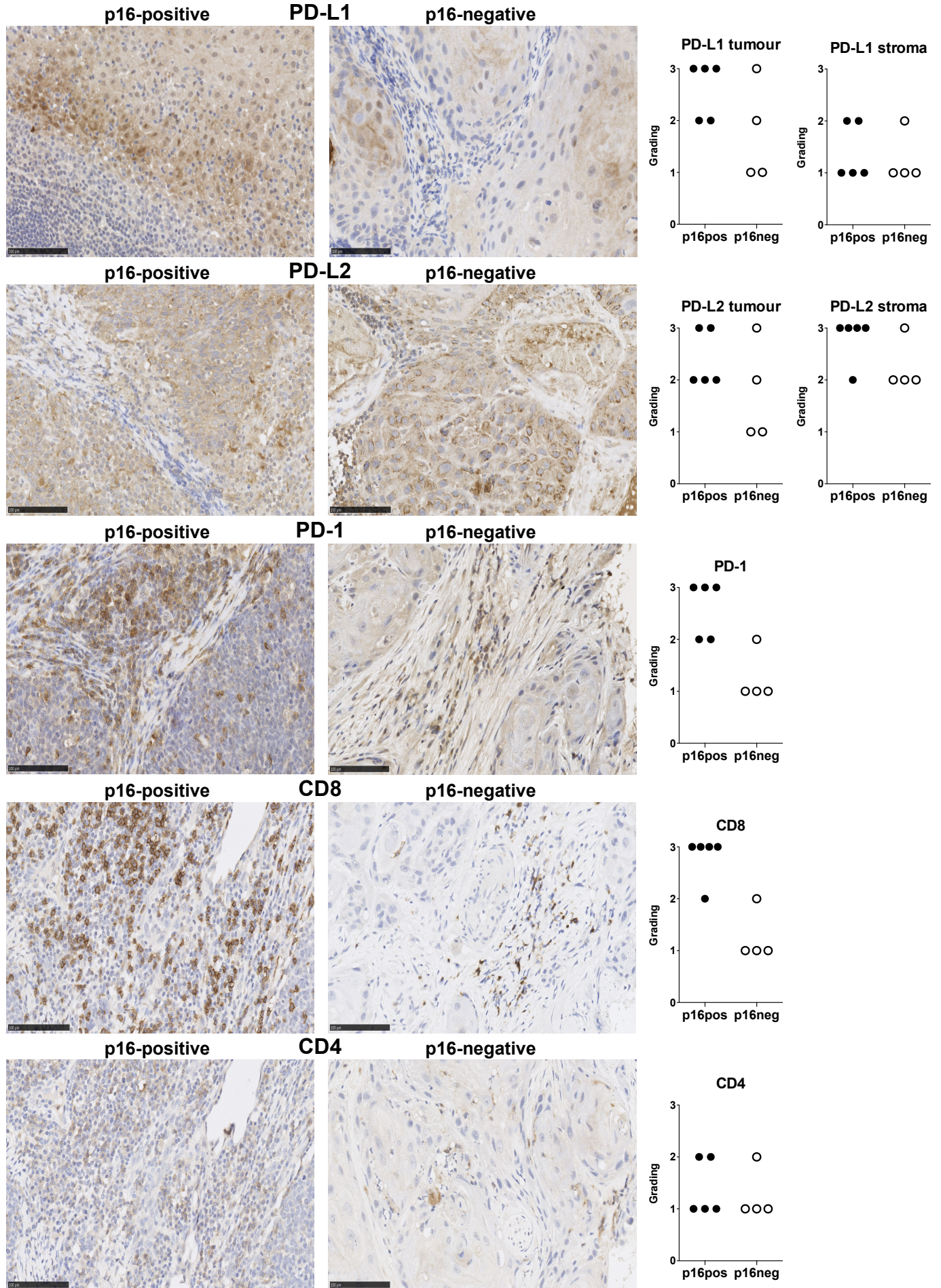


Figure 2

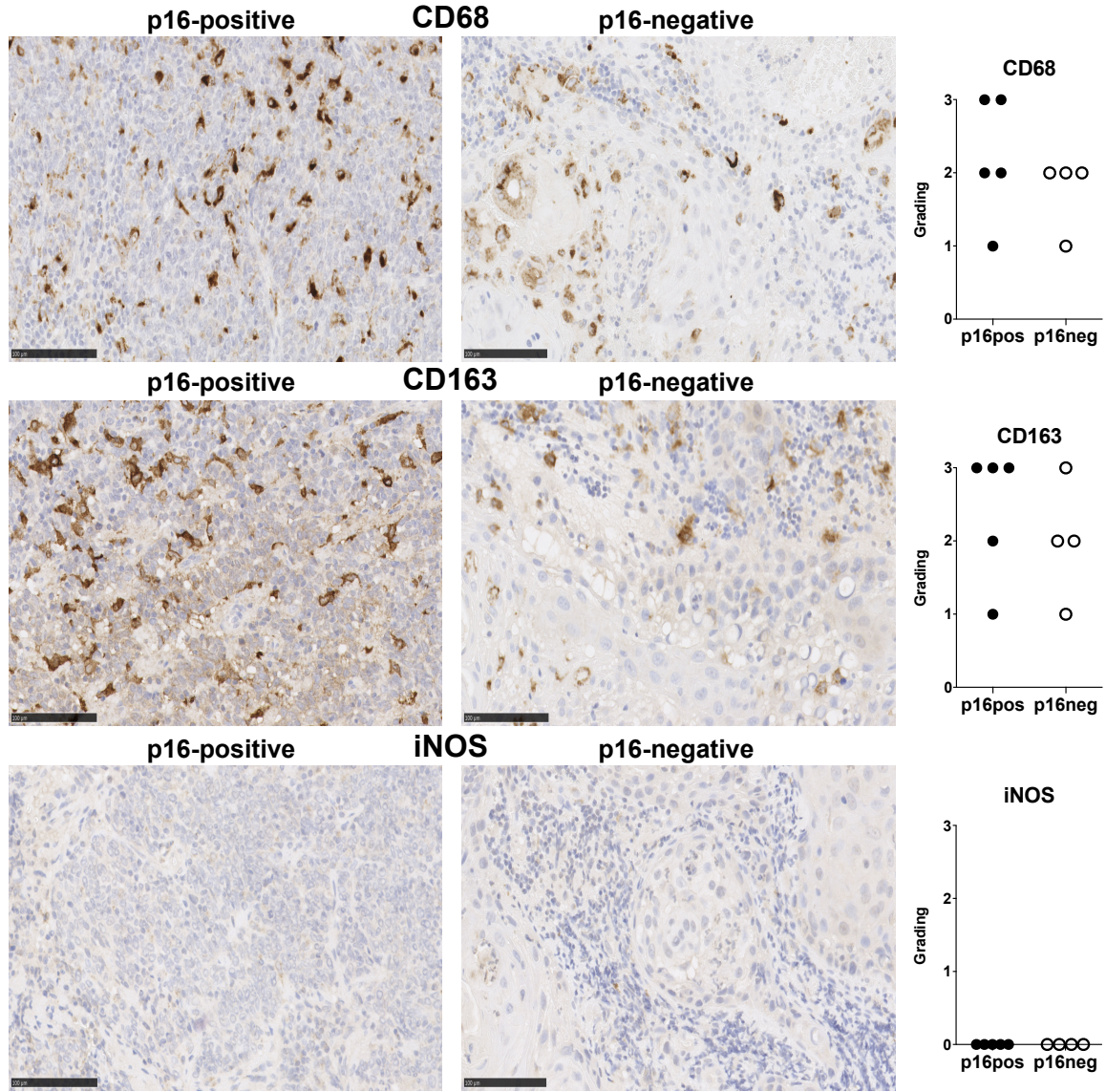


Figure 3

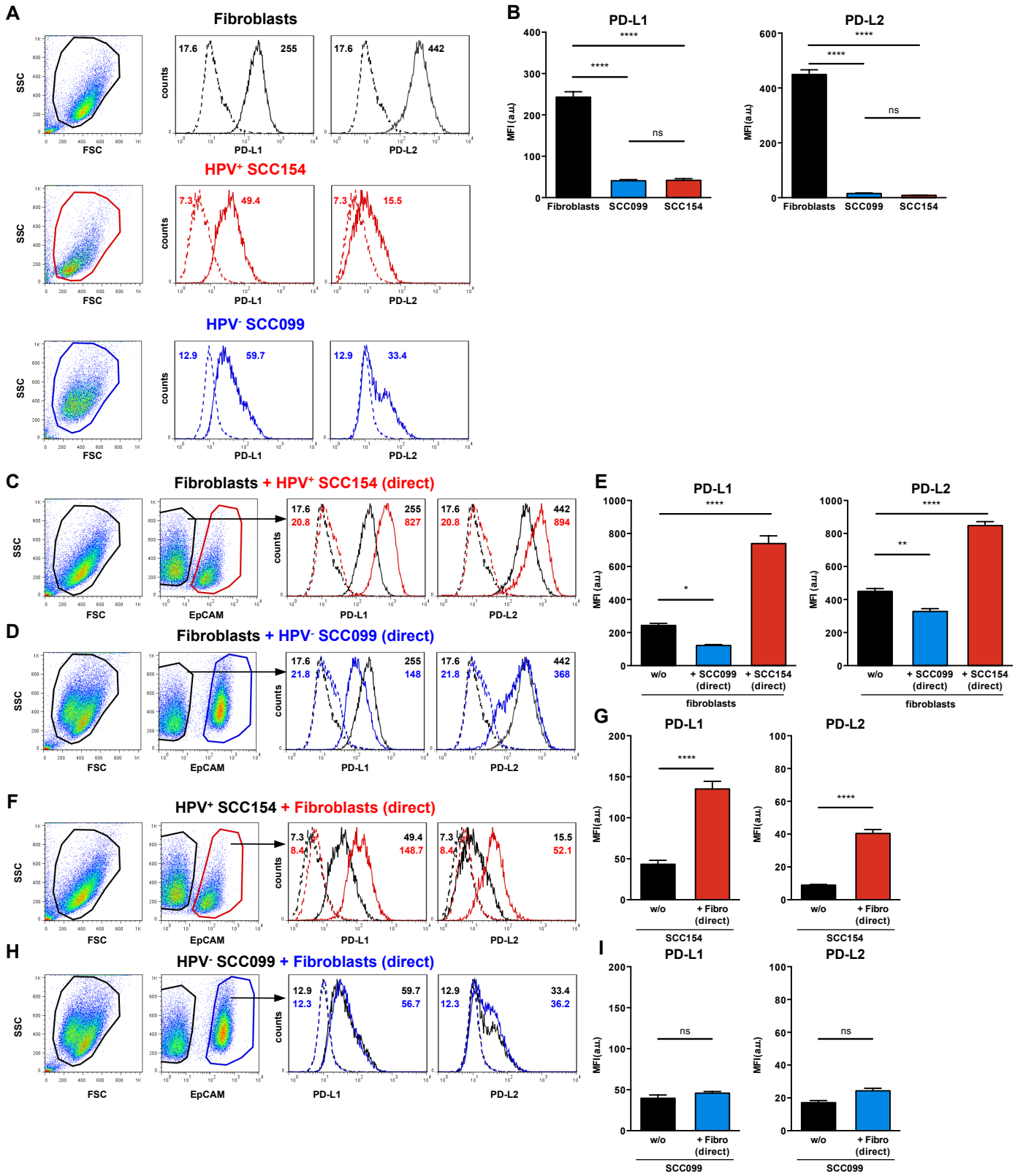


Figure 4

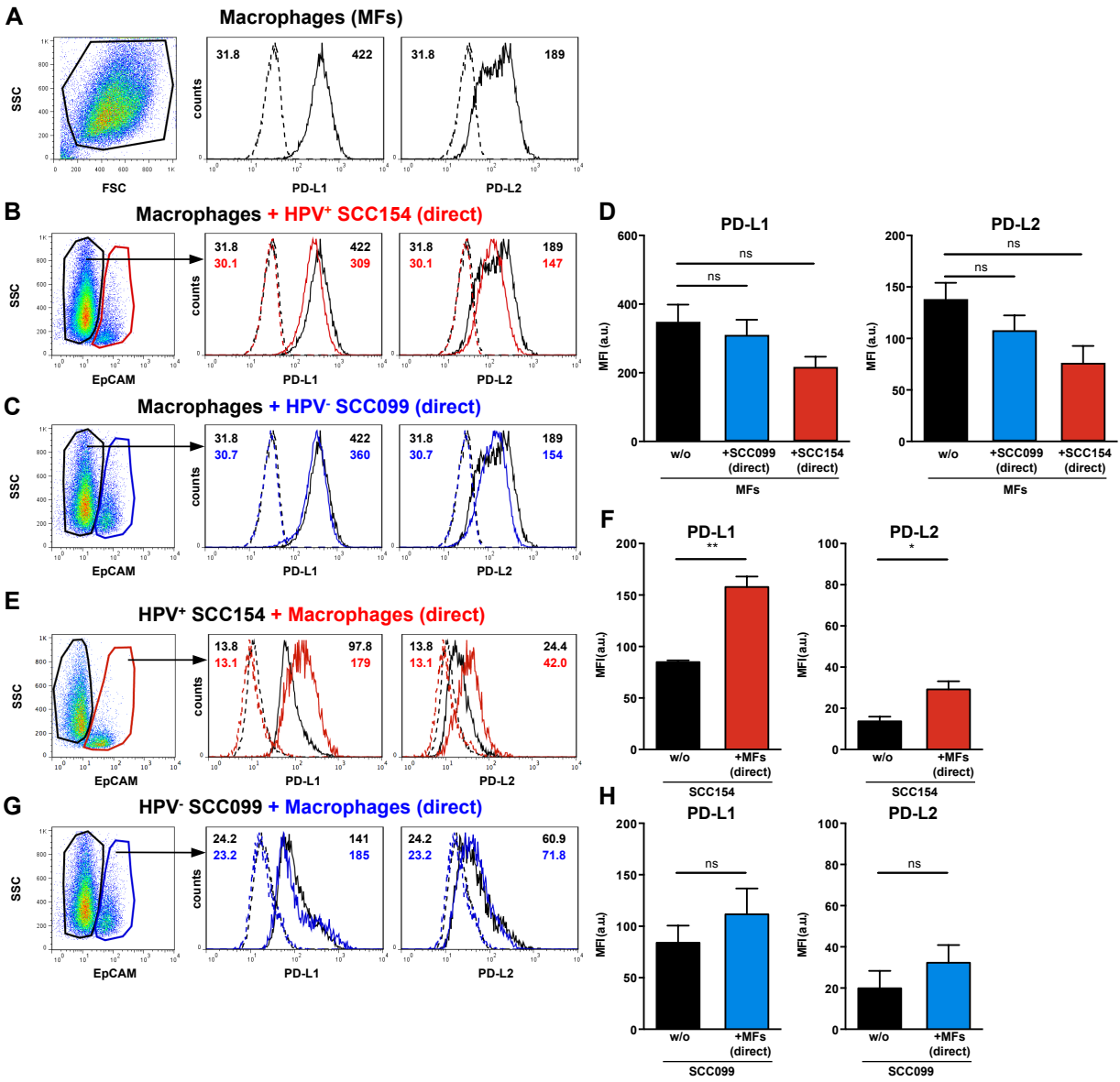
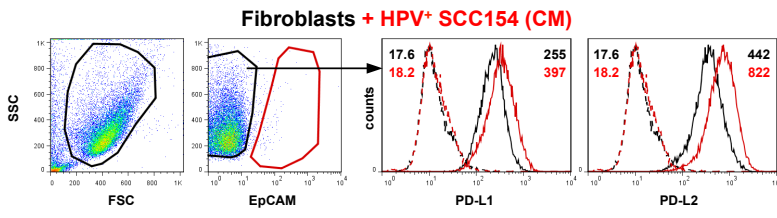
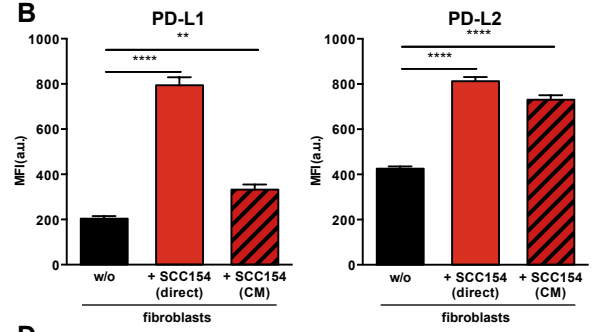


Figure 5

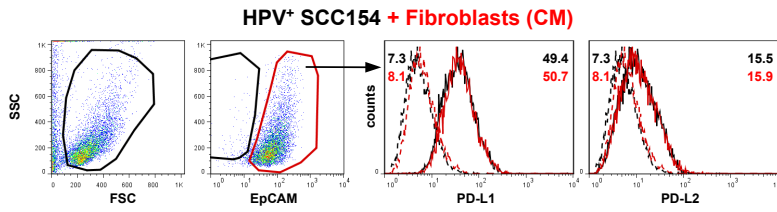
A



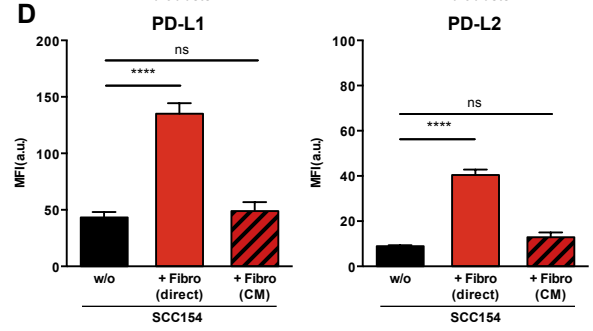
B



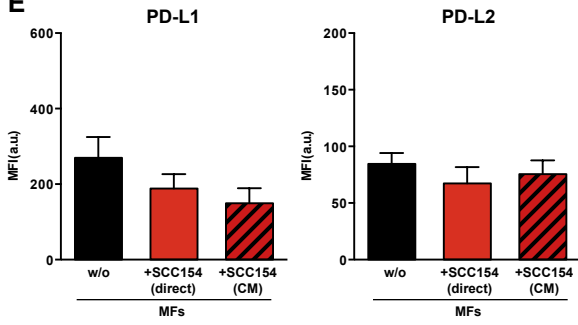
C



D



E



F

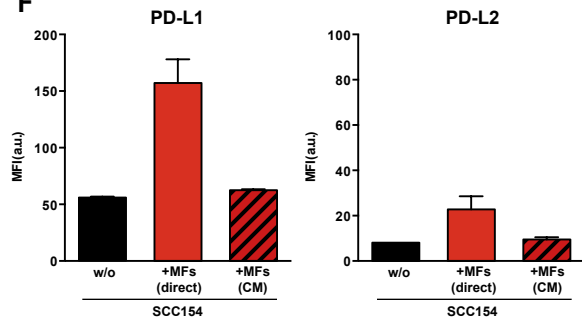


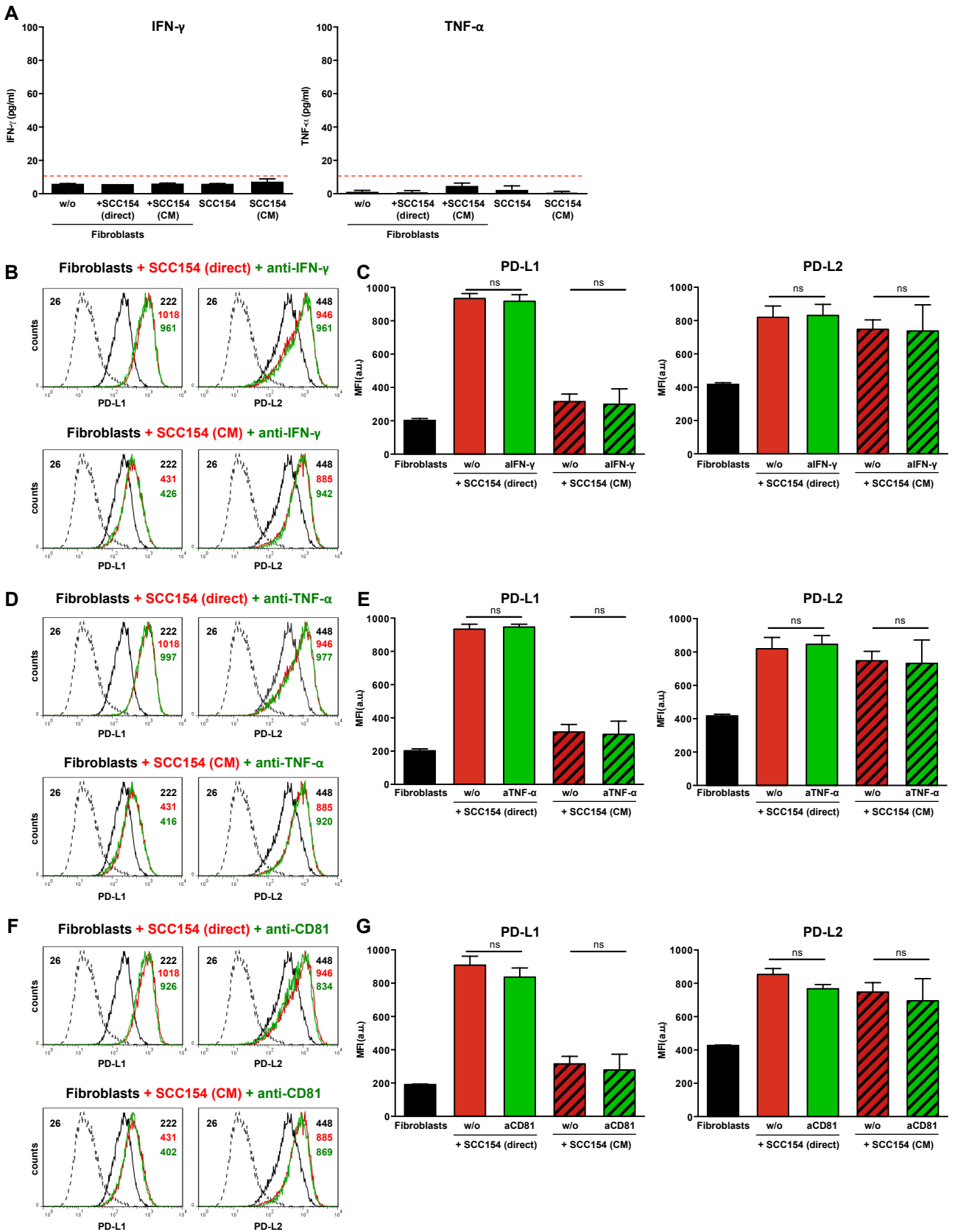
Figure 6

Figure 7

